J Musculoskelet Neuronal Interact 2026; 26(2):301-310

Journal of Musculoskeletal and Neuronal Interactions JMNI

Original Article

Astragalus Polysaccharides Attenuate LPS-Induced Degenerative Responses in Primary Rat Chondrocytes linked to the NLRP3/CASPASE-1 Axis

Xiaowei Jiang[1], Xin Ye[1], Taoye Li[1], Zhengfeng Mei[1], Yichun Zhang[1]

[1]Department of Orthopedics, Hangzhou Third People's Hospital, Hangzhou, Zhejiang, China

Abstract

Objectives: Cartilage degeneration is a key pathological change in osteoarthritis (OA). This study investigated the mechanism by which Astragalus polysaccharides (APS) alleviate cartilage degeneration. **Methods:** Primary rat articular chondrocytes were isolated, and a cell degeneration model was induced with lipopolysaccharide (LPS). Different concentrations of APS (100, 200, 400 mg/L) were tested, and NLR family pyrin domain containing 3 (NLRP3)-knockdown chondrocytes were generated. Cell viability (CCK-8 metabolic activity), levels of inflammatory factors, and gene and protein levels of markers associated with cartilage degeneration (including Acan, Adamts5, Nlrp3, and Caspase-1) were measured. **Results:** APS at different concentrations improved cell viability (CCK-8) of LPS-induced chondrocytes, inhibited the inflammatory cytokines interleukin-1β (IL-1β) and IL-18, upregulated Acan, and downregulated Adamts5, Nlrp3, and Caspase-1. Nlrp3 knockdown produced similar effects to APS, improving chondrocyte degeneration *in vitro*. **Conclusion:** APS alleviates LPS-induced degenerative responses in primary rat chondrocytes, and its protective effect is associated with modulation of the NLRP3/CASPASE-1 axis.

Keywords: Articular Cartilage Degeneration, Astragalus Polysaccharides, Caspase-1, NLR Family Pyrin Domain Containing 3, Osteoarthritis

Introduction

Osteoarthritis (OA), a common chronic joint disease, seriously affects the quality of life of many patients worldwide[1]. With population aging, the incidence of OA is increasing year by year, placing a heavy burden on society and families[1,2]. The main pathological features of OA include articular cartilage degeneration, subchondral bone remodeling, and synovial inflammation, among which articular cartilage degeneration is a core link in disease progression[3]. Articular cartilage is a highly specialized connective tissue whose main function is to cushion joint loading and reduce friction, thereby ensuring normal joint movement[4]. However, in patients with OA, multiple factors—such as abnormal mechanical stress, inflammatory mediator release, and imbalance of extracellular matrix metabolism—lead to gradual cartilage degradation; the number and function of chondrocytes are affected, ultimately resulting in joint dysfunction[5,6].

In recent years, the NLR family pyrin domain containing 3 (NLRP3)/CASPASE-1 axis has been found to play a key role in articular cartilage degeneration[7]. The NLRP3 inflammasome is a multiprotein complex that, upon activation, recruits and activates CASPASE-1 [8]. On the one hand, activated CASPASE-1 promotes the maturation and release of inflammatory cytokines such as interleukin-1β (IL-1β) and IL-18, leading to a strong inflammatory response; on the other hand, it can also induce apoptosis, accelerate the loss of articular chondrocytes, and further promote cartilage degeneration[9,10]. Therefore, inhibiting the activation of the NLRP3/CASPASE-1 axis is a promising strategy for the treatment of OA.

Based on the development of standardization in

The authors have no conflict of interest.

Corresponding author: Xin Ye, Department of Orthopedics, Hangzhou Third People's Hospital, No. 38, Xihu Avenue, Shangcheng District, Hangzhou City, Zhejiang Province 310009, China
E-mail: yexin_yx456@163.com

Edited by: G. Lyritis
Accepted 28 January 2026

traditional Chinese medicine and proposals for future work, Astragalus polysaccharides (APS)—an important component of polysaccharides extracted from *Astragalus radix* (the root of *Astragalus membranaceus*)—are worthy of further investigation to promote the application and development of active-component research in traditional Chinese medicine[11,12]. Modern pharmacological studies have shown that APS has a wide range of biological activities, including immunomodulatory, anti-inflammatory, antioxidant, and anti-fatigue effects[13]. In the OA field, several studies have reported that APS can alleviate OA symptoms, improve joint function, and exert a protective effect on articular cartilage[14]. In addition, studies in other diseases (e.g., allergic rhinitis) have found that APS can inhibit activation of the NLRP3 inflammasome, thereby reducing inflammation[15]. Considering the important role of the NLRP3/CASPASE-1 signaling pathway in cartilage degeneration and the potential of APS to impede NLRP3 inflammasome activation, we hypothesized that APS may mitigate articular cartilage degeneration by modulating the NLRP3/CASPASE-1 signaling pathway.

The impact of APS on articular cartilage degeneration and its mode of action remain incompletely defined. The objective of this study was to create an *in vitro* LPS-stimulated chondrocyte model, investigate the protective effects of APS on articular cartilage degeneration, and examine its potential role in inhibiting the NLRP3/CASPASE-1 signaling pathway, thereby providing a theoretical foundation for the application of APS in OA treatment.

Materials and Methods

Animals

Three 4-week-old male Sprague–Dawley (SD) rats (70–90 g) were supplied by Hangzhou Medical College (Hangzhou, China). After a one-week acclimation period, experiments were conducted. Animals were housed under specific pathogen-free (SPF) conditions at 23 ± 1 °C with a 12-h light/12-h dark cycle and *ad libitum* access to standard chow and water. All animal procedures were performed at Zhejiang Baiyue Biotechnology Co., Ltd.

Primary Culture of Rat Chondrocytes

Primary chondrocytes were isolated from 4-week-old rats and characterized as previously described[16]. The isolation procedure followed the referenced methods[16]. Rats were euthanized with an overdose of anesthetic (P3761, Sigma-Aldrich, St. Louis, MO, USA). Fur was removed with surgical scissors, and both knee joints were harvested. After immersion in 75% ethanol (C06915600, Nanjing Reagent, Nanjing, China), rats were placed on a clean surface. Following three phosphate-buffered saline (PBS; ST341, Beyotime, Shanghai, China) washes to remove residual hair, the knee joint was opened with a blade and the transparent articular cartilage was excised. After three PBS washes, cartilage was cut into ~1-mm^3 pieces and incubated at 37 °C in 0.2% type II collagenase (17101015, Thermo Fisher, Waltham, MA, USA) for 2 h. The digestion mixture was transferred to a 15-mL centrifuge tube and centrifuged at 1000 rpm for 3 min. The supernatant was discarded, and the cell pellet was resuspended in medium containing 10% fetal bovine serum (FBS; A5256701, Thermo Fisher, Waltham, MA, USA). Cells were plated and cultured at 37°C in a 5% CO_2 incubator (Forma Steri-Cult, Thermo Fisher, Waltham, MA, USA). Primary chondrocytes were maintained in Dulbecco's Modified Eagle Medium (DMEM; PM150312A, Pricella, Wuhan, China) with 10% FBS. Passage-2 (P2) chondrocytes were used for subsequent experiments. Primary rat chondrocytes were validated by type II collagen immunofluorescence and Toluidine blue staining[17].

Establishment and Grouping of Cell Degeneration Models

First, the effects of different concentrations of APS (10, 25, 50, 100, 200, 400 mg/L; SA9790, Solarbio, Beijing, China) on cell viability were assessed using the Cell Counting Kit-8 (CCK-8) assay. APS was characterized as follows: purity ≥90% (UV), average molecular weight 254.69 kDa with a narrow distribution (HPGPC), and endotoxin level checked using an endotoxin testing kit. The APS solution was confirmed to be endotoxin-free (endotoxin <0.5 EU/mL). The chondrocyte degeneration model was induced with 1 μg/mL lipopolysaccharide (LPS; ST1470, Beyotime, Shanghai, China) for 24 h[18]. Cells in optimal condition were then allocated to groups: control (conventional culture), LPS (1 μg/mL LPS), and APS intervention (1 μg/mL LPS + 100/200/400 mg/L APS). Treatments were applied for 24 h[19]. Based on these results, 200 mg/L APS was selected for the subsequent siRNA mechanistic experiments, whereas 100, 200, and 400 mg/L were used for the dose–response evaluation in the LPS model.

For Nlrp3 knockdown, chondrocytes were transfected with small interfering RNA targeting Nlrp3 (siNlrp3-1, 5′-GCACGTCTAATCTCTCCATGG-3′; siNlrp3-2, 5′-GGAUCUUUGCAGCGAUCAATT-3′; Sequence ID: NM_001191642.1) or a negative-control siRNA (siNC, 5′-TTCTCCGAACGTGTCACGT-3′) (GenePharma, China). Transfections were performed with Lipofectamine 3000 (L3000001, Invitrogen, Carlsbad, CA, USA) at a final siRNA concentration of 50 nM. Transfection efficiency was evaluated by quantitative real-time PCR (qRT-PCR). Cells were divided into the following groups: control (conventional culture), LPS + siNC (siNC + 1 μg/mL LPS), LPS + siNlrp3 (Nlrp3 knockdown + 1 μg/mL LPS), LPS + siNC + APS (siNC + 1 μg/mL LPS + 200 mg/L APS), and LPS + siNlrp3 + APS (Nlrp3 knockdown + 1 μg/mL LPS + 200 mg/L APS).

CCK-8

During logarithmic growth, 5,000 cells per well were seeded into 96-well plates (167008, Thermo Fisher,

Table 1. Primers used for qRT-PCR.

Target Gene	Amplicon sizes	Efficiency (%)	Forward Primer (5'-3')	Reverse Primer (5'-3')
Gapdh	63	98.5	GCCAGCCTCGTCTCATAGACA	GTCCGATACGGCCAAATCC
Acan	175	96.2	GACACCCCTACCCTTGCTTC	GGTCGATCTCACACAGGTCC
Adamts5	222	95.8	AGTACAGTTTGCCTACCGCC	AGGACACCTGCGTATTTGGG
Nlrp3	391	99.5	TGCATGCCGTATCTGGTTGT	ACCTCTTGCGAGGGTCTTTG
Caspase-1	108	99.7	TGGAAATGTGCCATCTTCTTT	TCAGCTCCATCAGCTGAAAC

Note: Despite the relatively long Nlrp3 amplicon (391 bp), the assay satisfied acceptance criteria for specificity (single melt-curve peak) and amplification efficiency (standard curve-derived).

Table 2. Antibodies used for Western blotting.

Antibodies	Species	Molecular weight	Clonality	Clones	Dilutions	Catalog numbers	RRID	Vendor
NLRP3	Rabbit	118 kDa	Monoclonal	EPR23094-1	1:1000	ab263899	AB_2889890	Abcam, UK
CASPASE-1	Mouse	45 kDa	Monoclonal	D-3	1:500	sc-392736	–	SCBT, USA
ACAN	Rabbit	250 kDa	Monoclonal	EPR28034-86	1:1000	ab313636	AB_3166183	Abcam, UK
ADAMTS5	Rabbit	73 kDa	Polyclonal	–	1:250	ab41037	AB_2222327	Abcam, UK
GAPDH	Mouse	37 kDa	Monoclonal	6C5	1:1000	ab8245	AB_2107448	Abcam, UK
Goat Anti-Rabbit IgG H&L (HRP)	Goat	–	Polyclonal	–	1:2000	ab6721	AB_955447	Abcam, UK
Goat Anti-Mouse IgG H&L (HRP)	Goat	–	Polyclonal	–	1:2000	ab6789	AB_955439	Abcam, UK

Waltham, MA, USA) and incubated overnight in a 5% CO_2 incubator. After cell attachment, treatment was applied according to the experimental groups. An equal volume of sterile double-distilled water (vehicle for APS) was added to the control and to all groups without APS to ensure identical treatment volumes across groups. The osmolality and pH of the vehicle-containing medium were verified to be within physiological ranges (295 ± 5 mOsm/kg; pH 7.35 ± 0.05). Six wells were allocated per group. Plates were incubated for 24 h, after which 10 µL of CCK-8 reagent (C0038, Beyotime, Shanghai, China) was added to each well and incubated for 2 h. Absorbance at 450 nm was recorded using a microplate reader (Varioskan LUX, Thermo Fisher, Waltham, MA, USA).

Enzyme Linked Immunosorbent Assay (ELISA)

The concentrations of interleukin-1β (IL-1β) and IL-18 in cell-culture supernatants were quantified using commercial sandwich ELISA kits (IL-1β, PI303; IL-18, PI555; Beyotime, Shanghai, China) in strict accordance with the manufacturer's protocols. Briefly, after treatments, supernatants were collected and centrifuged at 1,000 × g for 10 min to remove debris. Assays were performed on the provided antibody-precoated 96-well plates.

A standard curve was generated for each assay using the supplied recombinant cytokine standards serially diluted in the kit diluent. Undiluted supernatants and standards were added in duplicate (100 µL/well) and incubated at room temperature (RT) for 120 min. After washing, 100 µL of biotin-conjugated detection antibody was added and incubated for 60 min at RT. Following another wash, 100 µL of horseradish peroxidase (HRP)–labeled streptavidin was added and incubated for 20 min at RT, protected from light. After a final wash, 100 µL of tetramethylbenzidine (TMB) substrate was added and incubated for 20 min in the dark for color development. The reaction was stopped by adding 50 µL of stop solution, and absorbance was read immediately at 450 nm using a Varioskan LUX microplate reader (Thermo Fisher, Waltham, MA, USA; RRID: SCR_026792).

Cytokine concentrations were calculated by interpolating the mean absorbance of duplicate wells from a 4-parameter logistic (4-PL) standard curve. Results are expressed as picograms per milliliter (pg/mL).

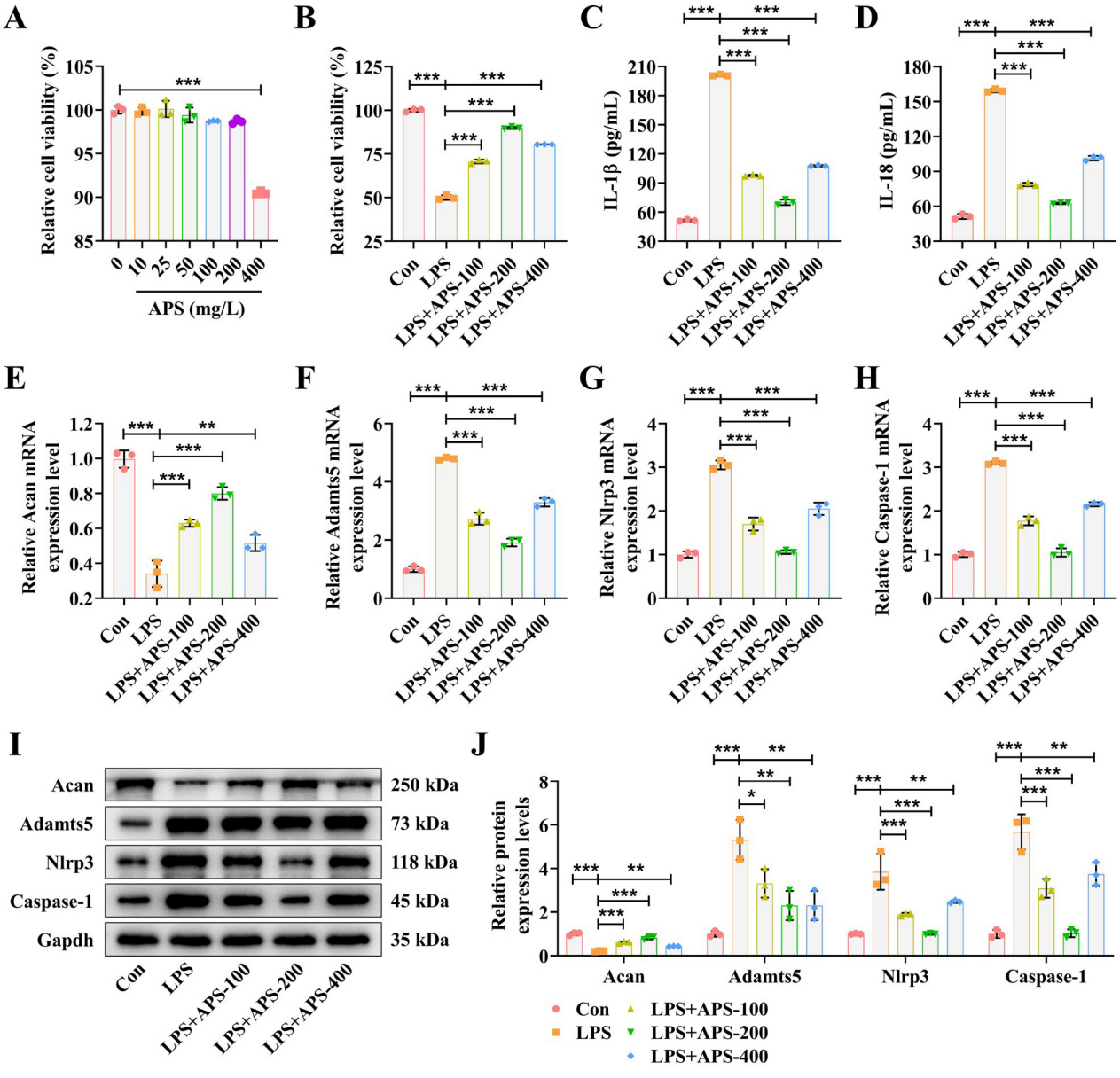

Figure 1. Treatment with astragalus polysaccharides (APS) at different concentrations could improve chondrocyte degeneration. (A) The effects of APS at different concentrations (10, 25, 50, 100, 200, 400 mg/L) on chondrocyte viability were detected by Cell Counting Kit-8 (CCK-8). (B) The effect of APS (100, 200, 400 mg/L) on cell viability (CCK-8) of lipopolysaccharide (LPS)-induced chondrocytes was detected by CCK-8. (C-D) The levels of inflammatory cytokines were detected by enzyme linked immunosorbent assay (ELISA). (E–H) mRNA levels (qRT-PCR). (I–J) protein levels (Western blot). GAPDH was used as the loading control. Each experiment was repeated 3 times (biological replicate). Biological replicates represent independent chondrocyte isolations from different animals (n=3), with technical duplicates per assay.*P<0.05, **P<0.01, ***P<0.001.

qRT-PCR

Total RNA was extracted by adding TRIzol reagent (15596026, Invitrogen, Carlsbad, CA, USA) to the cells. Reverse transcription was performed to generate cDNA using the High-Capacity cDNA Reverse Transcription Kit (4368813, Applied Biosystems, Foster City, CA, USA). Gene-specific primers for Acan, Adamts5, Nlrp3, Caspase-1, and Gapdh (Sangon Biotech, Shanghai, China) were used for quantitative PCR. Reactions were assembled according to the manufacturer's instructions for SYBR™ GreenER™ qPCR SuperMix (1176202K, Invitrogen) in a total volume of 50 µL. Amplification was run on a QuantStudio™ 3 Real-Time PCR System (A28137, Applied Biosystems) using the instrument's

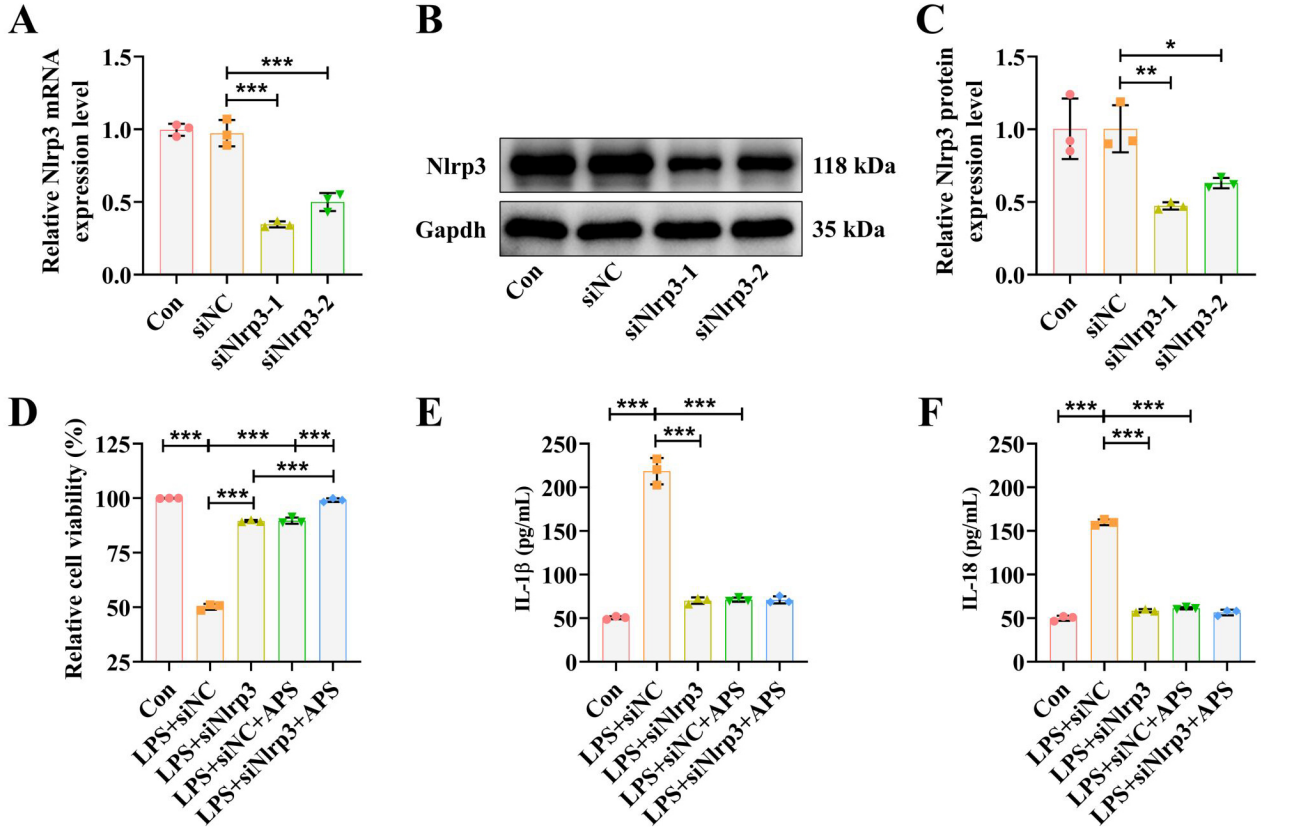

Figure 2. APS improved LPS-induced degenerative responses and was associated with reduced NLRP3/CASPASE-1 expression. (A) Nlrp3 mRNA (qRT-PCR); (B–C) NLRP3 protein (Western blot). GAPDH was used as the loading control. (D) CCK-8 was used to assess cell viability (metabolic activity). (E-F) The levels of inflammatory cytokines were detected by ELISA. Each experiment was repeated 3 times (biological replicate). Biological replicates represent independent chondrocyte isolations from different animals (n=3), with technical duplicates per assay. *P<0.05, **P<0.01, ***P<0.001.

standard cycling protocol. Primer sequences used in the qRT-PCR experiments are provided in Table 1.

Western blotting

Total protein was extracted from cells in radioimmunoprecipitation assay (RIPA) buffer (R0010, Solarbio, Beijing, China). Protein concentration was determined using the bicinchoninic acid (BCA) assay (BCA1, Sigma-Aldrich, St. Louis, MO, USA). Equal amounts of protein (20 μg per lane) were separated by sodium dodecyl sulfate–polyacrylamide gel electrophoresis (SDS-PAGE; P0012A, Beyotime, Shanghai, China) and transferred by wet transfer to polyvinylidene fluoride (PVDF) membranes (YA1700, Solarbio, Beijing, China). Membranes were blocked with 5% skim milk at room temperature for 1.5 h and then incubated with primary antibodies (listed in Table 2) overnight at 4 °C. The CASPASE-1 antibody used detects total/pro-caspase-1 (≈45 kDa); cleaved caspase-1 was not assessed. The following day, membranes were incubated with the appropriate secondary antibody for 2 h at room temperature. Bands were visualized using a gel imaging system (ChampGel® 7800, SINSAGE, Beijing, China), and band gray values were quantified in ImageJ. The relative level of each target protein was normalized to GAPDH.

Statistical Analysis

Data are expressed as mean ± standard deviation (SD). Biological replicates represent independent primary chondrocyte isolations from different animals (n=3); technical replicate wells were averaged per biological replicate before statistical testing. Normality was assessed using the Shapiro–Wilk test, and homoscedasticity using Levene's test. Comparisons among multiple groups were performed by one-way analysis of variance (ANOVA) followed by Šidák's post hoc test. Statistical analyses were conducted in GraphPad Prism 8.0 (GraphPad Software, San Diego, CA, USA). A value of $P < 0.05$ was considered statistically significant.

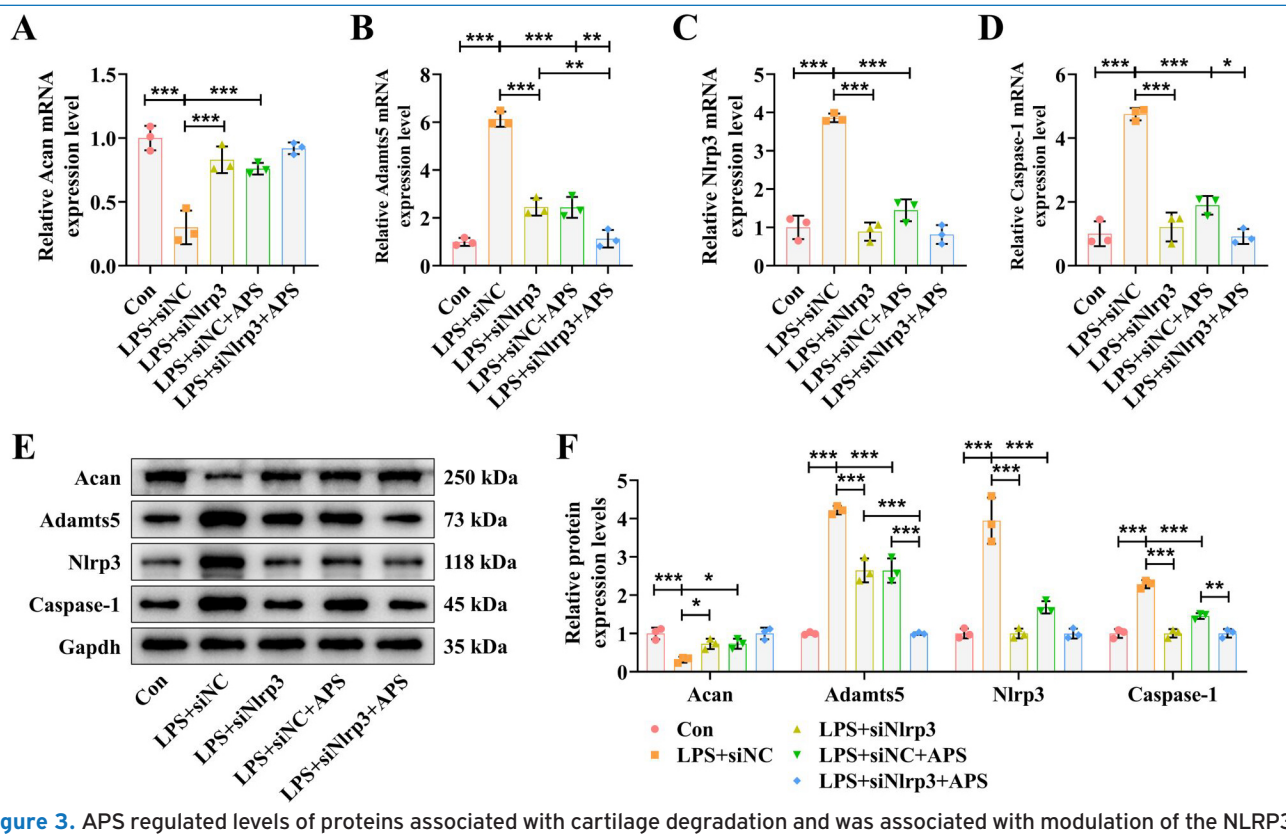

Figure 3. APS regulated levels of proteins associated with cartilage degradation and was associated with modulation of the NLRP3/CASPASE-1 axis. (A–D) *Acan, Adamts5, Nlrp3, Caspase-1 mRNA* (qRT-PCR); (E–F) ACAN, ADAMTS5, NLRP3, CASPASE-1 protein (Western blot). GAPDH was used as the loading control. Each experiment was repeated 3 times (biological replicate). Biological replicates represent independent chondrocyte isolations from different animals (n=3), with technical duplicates per assay. **P*<0.05, ***P*<0.01, ****P*<0.001.

Results

Different concentrations of APS ameliorate LPS-induced chondrocyte degeneration and are associated with modulation of NLRP3/CASPASE-1 axis

Cell Counting Kit-8 (CCK-8) results showed that 400 mg/L APS significantly reduced chondrocyte viability (Figure 1A, P < 0.001), whereas 200 mg/L APS had no significant effect (Figure 1A). Therefore, 100 and 200 mg/L were selected as non-cytotoxic (or low-to-moderate) concentrations, and 400 mg/L was retained as a high-dose condition to evaluate whether APS confers protection under LPS-induced inflammatory stress and to define the upper boundary of the dose–response. Accordingly, follow-up experiments used 100, 200, and 400 mg/L APS. Different APS concentrations significantly improved the LPS-suppressed cell viability (CCK-8) of chondrocytes (Figure 1B, P < 0.01). Regarding inflammatory mediators, LPS increased IL-1β and IL-18 in chondrocytes, whereas APS reduced IL-1β and IL-18 levels (Figure 1C–D, P < 0.001). Subsequently, we quantified mRNA (Figure 1E–H) and protein (Figure 1I–J) levels. In LPS-stimulated primary rat chondrocytes, Acan mRNA and ACAN protein decreased, whereas Adamts5/ADAMTS5, Nlrp3/NLRP3, and Caspase-1/CASPASE-1 increased. Treatment with APS (as indicated in Figure 1) partially reversed these changes, increasing Acan/ACAN and decreasing Adamts5/ADAMTS5, Nlrp3/NLRP3, and Caspase-1/CASPASE-1 (Figure 1E–J; P < 0.01).

The protective role of APS is linked to NLRP3/CASPASE-1 axis

To explore the mechanism by which APS alleviates cartilage-related degeneration *in vitro* in primary rat chondrocytes, we generated Nlrp3-knockdown chondrocytes (Figure 2A–C, *P* < 0.05) and treated cells with 200 mg/L APS. The siRNA with higher silencing efficiency (siNlrp3-1) was selected for subsequent experiments. In CCK-8 viability assays, LPS significantly reduced viability compared with the control group (Figure 2D, P < 0.001). Both APS treatment and Nlrp3 knockdown increased cell viability (CCK-8 metabolic activity) and the combination of APS with siNlrp3 produced a more pronounced effect (Figure 2D, P < 0.001).

LPS increased the inflammatory cytokines IL-1β and IL-18 in chondrocytes (Figure 2E–F, $P < 0.001$). APS treatment or Nlrp3 knockdown reduced IL-1β and IL-18 (Figure 2E–F, $P < 0.001$), and APS + siNlrp3 did not differ significantly from APS alone or siNlrp3 alone for these cytokines (Figure 2E–F). Finally, in analyses of cartilage-degeneration markers, LPS decreased Acan and increased Adamts5, Nlrp3, and Caspase-1 relative to control (Figure 3A–F, $P< 0.001$). APS or Nlrp3 knockdown significantly reversed these LPS-induced changes—upregulating Acan and downregulating Adamts5, Nlrp3, and Caspase-1 (Figure 3A–F, $P < 0.01$). Notably, APS + siNlrp3 exerted a stronger effect on Adamts5 and Caspase-1 than APS alone, and the effect on Adamts5 was also greater than with siNlrp3 alone (Figure 3A–F, $P < 0.05$).

Discussion

The pathological process of OA mainly consists of articular cartilage degeneration, matrix degradation, and synovial inflammation, which eventually lead to joint injury, deformity, and dysfunction[20]. Numerous studies have shown that interactions among extracellular matrix proteases, inflammatory mediators, oxidative stress, and other active factors drive the onset and progression of OA, and that extracellular matrix degradation is a principal cause of chondrocyte death and dysfunction, thereby accelerating articular cartilage degeneration[21]. ACAN, a crucial component of the cartilage extracellular matrix, preserves cartilage elasticity and resistance to stress when present in sufficient amounts[22]. Down-regulation of Acan mRNA signifies loss of cartilage matrix components, compromising structural integrity and thereby accelerating cartilage degradation[23]. ADAMTS5 is a proteolytic enzyme that specifically degrades ACAN; increased ADAMTS5 promotes destruction of the cartilage matrix and is a significant contributor to cartilage degeneration[24,25].

The NLRP3/CASPASE-1 signaling pathway plays a central role in cartilage degeneration[26]. LPS is widely used to induce inflammatory/degenerative responses in chondrocytes and can promote upregulation of inflammasome pathway components. The NLRP3 inflammasome regulates CASPASE-1 activation and drives inflammatory responses, and it is a therapeutic target for various inflammatory diseases[27]. When pattern-recognition receptors are stimulated, signaling leads to up-regulation of NLRP3 protein and the precursors of IL-1β and IL-18. The subsequent accumulation of NLRP3 protein, apoptosis-associated speck-like protein, and pro-CASPASE-1 forms active NLRP3 inflammasomes[28]. Pro-CASPASE-1 is then cleaved to the active form CASPASE-1, which promotes the maturation and secretion of IL-1β and IL-18 and can trigger pyroptosis[8,29].

APS is a principal bioactive constituent of *Astragalus* with antioxidant, anti-inflammatory, and immunomodulatory activities, and it has been widely examined in clinical research across multiple diseases[30–32]. In chondrocytes, APS has been reported to reduce reactive-oxygen-species–induced oxidative stress, thereby lowering pro-apoptotic factor expression and restoring chondrocyte function[33]. In this study, APS showed a protective effect in degenerative chondrocytes. APS increased cell viability (CCK-8 metabolic activity) in LPS-induced degenerative chondrocytes, providing a cellular basis for cartilage repair. In terms of inflammation, LPS significantly upregulated inflammatory factors in degenerative cells, whereas APS effectively downregulated these cytokines and reduced inflammatory damage to chondrocytes. Notably, APS exhibited a biphasic dose–response, a phenomenon commonly observed with natural bioactive compounds[34]. In our experiments, 400 mg/L APS produced a modest cytotoxic effect in normal chondrocytes, yet the same dose conferred significant protection against LPS-induced injury—likely because anti-inflammatory and cytoprotective effects outweighed minor toxicity under stress conditions.

The regulatory effects of APS on cartilage degeneration–related proteins and the NLRP3/CASPASE-1 axis were of particular interest. APS treatment markedly increased ACAN protein levels while decreasing ADAMTS5, NLRP3, and CASPASE-1 protein levels. Results from the Nlrp3 knockdown experiments, which phenocopied the effects of APS, support the hypothesis that the protective action of APS is linked to the NLRP3/CASPASE-1 axis. Notably, the observation that Nlrp3 knockdown produced similar protective effects and molecular changes suggests that APS exerts its effects, at least in part, through a mechanism associated with the NLRP3/CASPASE-1 axis. A previous study reported that, based on network pharmacology analysis, multiple active components of Simiao Yong'an Decoction act on multiple rheumatoid arthritis targets and exert a broad range of pharmacological effects[35]. In future work, a strategy combining network pharmacology with experimental verification could be used to further explore the mechanism by which APS alleviates articular cartilage degeneration, thereby supporting mechanistic research on active ingredients in traditional Chinese medicine.

In conclusion, this study provides evidence that Astragalus polysaccharides (APS) attenuate LPS-induced degenerative responses in primary rat chondrocytes. Collectively, the observed downregulation of pathway components and the phenocopying of APS effects by Nlrp3 knockdown suggest that APS acts, at least in part, through a mechanism associated with the NLRP3/CASPASE-1 axis. However, this study has limitations. Experiments were conducted only at the cellular level. Although the effects of APS on degenerative chondrocytes and the associated mechanisms can be characterized *in vitro*, this model does not fully recapitulate the complex physiological environment *in vivo*. Therefore, the *in vivo* efficacy of APS may be influenced by additional factors, including immune regulation and systemic metabolism. Future studies should verify the protective effects of APS on articular cartilage

degeneration in animal models and further investigate its *in vivo* mechanism of action and pharmacokinetic characteristics to provide a more comprehensive basis for the clinical application of APS in OA and other cartilage-degenerative diseases. In addition, the present study primarily relied on measurements of mRNA expression, total protein abundance, and downstream cytokine release. Future studies incorporating direct assessments of NLRP3/CASPASE-1 activation would be valuable to determine whether APS directly inhibits inflammasome assembly and activation.

Ethics Approval

All animal procedures were approved by the Ethics Committee of Zhejiang Baiyue Biotechnology Co., Ltd. (Approval No. ZJBYLA-IACUC-20240911) and were conducted in accordance with applicable institutional and national guidelines for the care and use of laboratory animals.

Authors' contributions

XJ and XY conceived and designed the study, and drafted the manuscript. XJ, XY, TL, ZM and YZ collected, analyzed and interpreted the experimental data. XY and TL revised the manuscript for important intellectual content. All authors read and approved the final manuscript.

Funding

This work was supported by the Zhejiang Province Traditional Chinese Medicine Science and Technology Project [grant number: 2024ZL731].

References

1. Molnar V, Matišić V, Kodvanj I, Bjelica R, Jeleč Ž, Hudetz D, Rod E, Čukelj F, Vrdoljak T, Vidović D, et al. Cytokines and Chemokines Involved in Osteoarthritis Pathogenesis. Int J Mol Sci. 2021;22(17):9208.
2. Knights AJ, Redding SJ, Maerz T. Inflammation in osteoarthritis: the latest progress and ongoing challenges. Curr Opin Rheumatol. 2023;35(2):128-134.
3. Vincent TL, Alliston T, Kapoor M, Loeser RF, Troeberg L, Little CB. Osteoarthritis Pathophysiology: Therapeutic Target Discovery may Require a Multifaceted Approach. Clin Geriatr Med. 2022;38(2):193-219.
4. Yao Q, Wu X, Tao C, Gong W, Chen M, Qu M, Zhong Y, He T, Chen S, Xiao G. Osteoarthritis: pathogenic signaling pathways and therapeutic targets. Signal Transduct Target Ther. 2023;8(1):56.
5. Cho Y, Jeong S, Kim H, Kang D, Lee J, Kang SB, Kim JH. Disease-modifying therapeutic strategies in osteoarthritis: current status and future directions. Exp Mol Med. 2021;53(11):1689-1696.
6. Hu W, Chen Y, Dou C, Dong S. Microenvironment in subchondral bone: predominant regulator for the treatment of osteoarthritis. Ann Rheum Dis. 2021;80(4):413-422.
7. Jin X, Dong X, Sun Y, Liu Z, Liu L, Gu H. Dietary Fatty Acid Regulation of the NLRP3 Inflammasome via the TLR4/NF-κB Signaling Pathway Affects Chondrocyte Pyroptosis. Oxid Med Cell Longev. 2022;2022:3711371.
8. Liu J, Jia S, Yang Y, Piao L, Wang Z, Jin Z, Bai L. Exercise induced meteorin-like protects chondrocytes against inflammation and pyroptosis in osteoarthritis by inhibiting PI3K/Akt/NF-κB and NLRP3/caspase-1/GSDMD signaling. Biomed Pharmacother. 2023;158:114118.
9. Bai H, Zhang Z, Liu L, Wang X, Song X, Gao L. Activation of adenosine A3 receptor attenuates progression of osteoarthritis through inhibiting the NLRP3/caspase-1/GSDMD induced signalling. J Cell Mol Med. 2022;26(15):4230-4243.
10. Fu J, Wu H. Structural Mechanisms of NLRP3 Inflammasome Assembly and Activation. Annu Rev Immunol. 2023;41:301-316.
11. Wang Y, Wang Y. Analysis of the development course of traditional Chinese medicine standardization and recommendations on future work. Guidelines and Standards in Chinese Medicine 2023;1(1):1-8.
12. Yuan J, Cheng K, Zhang X, Li C, Li B, Wang Z, Zheng Y. Exploring the Mechanism of Astragalus membranaceus in the Treatment of Post-Infectious Irritable Bowel Syndrome Based on Random Walk with Restart Algorithm and Experimental Validation. Journal of Experimental and Clinical Application of Chinese Medicine 2024; 5(2): 22-35.
13. Dong M, Li J, Yang D, Li M, Wei J. Biosynthesis and Pharmacological Activities of Flavonoids, Triterpene Saponins and Polysaccharides Derived from Astragalus membranaceus. Molecules. 2023;28(13):5018.
14. Xu J, Yu Y, Chen K, Wang Y, Zhu Y, Zou X, Xu X, Jiang Y. Astragalus polysaccharides ameliorate osteoarthritis via inhibiting apoptosis by regulating ROS-mediated ASK1/p38 MAPK signaling pathway targeting on TXN. Int J Biol Macromol. 2024;258(Pt 2):129004.
15. Xu J, Zhang Q, Li Z, Gao Y, Pang Z, Wu Y, Li G, Lu D, Zhang L, Li D. *Astragalus* Polysaccharides Attenuate Ovalbumin-Induced Allergic Rhinitis in Rats by Inhibiting NLRP3 Inflammasome Activation and NOD2-Mediated NF-κB Activation. J Med Food. 2021;24(1):1-9.
16. Chen J, Liu Z, Sun H, Liu M, Wang J, Zheng C, Cao X. MiR-203a-3p attenuates apoptosis and pyroptosis of chondrocytes by regulating the MYD88/NF-κB pathway to alleviate osteoarthritis progression. Aging (Albany NY). 2023;15(23):14457-14472.
17. Cao Y, Tang S, Nie X, Zhou Z, Ruan G, Han W, Zhu Z, Ding C. Decreased miR-214-3p activates NF-κB pathway and aggravates osteoarthritis progression, EBioMedicine 2021;65:103283.
18. Guo Q, Zhang M, Dong Y, Liu K, Wang D, Zheng J. Isobavachalcone ameliorates the progression of osteoarthritis by suppressing NF-κB signaling pathway. Int Immunopharmacol. 2023;119:110102.

19. Dong N, Li X, Xue C, Zhang L, Wang C, Xu X, Shan A. Astragalus polysaccharides alleviates LPS-induced inflammation via the NF-κB/MAPK signaling pathway. J Cell Physiol. 2020;235(7-8):5525-5540.
20. Salman LA, Ahmed G, Dakin SG, Kendrick B, Price A. Osteoarthritis: a narrative review of molecular approaches to disease management. Arthritis Res Ther. 2023;25(1):27.
21. Nedunchezhiyan U, Varughese I, Sun AR, Wu X, Crawford R, Prasadam I. Obesity, Inflammation, and Immune System in Osteoarthritis. Front Immunol. 2022;13:907750.
22. Bay-Jensen AC, Mobasheri A, Thudium CS, Kraus VB, Karsdal MA. Blood and urine biomarkers in osteoarthritis - an update on cartilage associated type II collagen and aggrecan markers. Curr Opin Rheumatol. 2022;34(1):54-60.
23. Lu R, He Z, Zhang W, Wang Y, Cheng P, Lv Z, Yuan X, Guo F, You H, Chen AM, Hu W. Oroxin B alleviates osteoarthritis through anti-inflammation and inhibition of PI3K/AKT/mTOR signaling pathway and enhancement of autophagy. Front Endocrinol (Lausanne). 2022;13:1060721.
24. Li T, Peng J, Li Q, Shu Y, Zhu P, Hao L. The Mechanism and Role of ADAMTS Protein Family in Osteoarthritis. Biomolecules. 2022;12(7):959.
25. Fang Y, Lou C, Lv J, Zhang C, Zhu Z, Hu W, Chen H, Sun L, Zheng W. Sipeimine ameliorates osteoarthritis progression by suppression of NLRP3 inflammasome-mediated pyroptosis through inhibition of PI3K/AKT/NF-κB pathway: An *in vitro* and *in vivo* study. J Orthop Translat. 2024;46:1-17.
26. Chen Y, Liu Y, Jiang K, Wen Z, Cao X, Wu S. Linear ubiquitination of LKB1 activates AMPK pathway to inhibit NLRP3 inflammasome response and reduce chondrocyte pyroptosis in osteoarthritis. J Orthop Translat. 2022;39:1-11.
27. Liu W, Liu A, Li X, Sun Z, Sun Z, Liu Y, Wang G, Huang D, Xiong H, Yu S, Zhang X, Fan C. Dual-engineered cartilage-targeting extracellular vesicles derived from mesenchymal stem cells enhance osteoarthritis treatment via miR-223/NLRP3/pyroptosis axis: Toward a precision therapy. Bioact Mater. 2023;30:169-183.
28. Han X, Lin D, Huang W, Li D, Li N, Xie X. Mechanism of NLRP3 inflammasome intervention for synovitis in knee osteoarthritis: A review of TCM intervention. Front Genet. 2023;14:1159167.
29. Zhang X, Wang Q, Cao G, Luo M, Hou H, Yue C. Pyroptosis by NLRP3/caspase-1/gasdermin-D pathway in synovial tissues of rheumatoid arthritis patients. J Cell Mol Med. 2023;27(16):2448-2456.
30. Zhang J, Feng Q. Pharmacological Effects and Molecular Protective Mechanisms of Astragalus Polysaccharides on Nonalcoholic Fatty Liver Disease. Front Pharmacol. 2022;13:854674.
31. Yang Q, Meng D, Zhang Q, Wang J. Advances in research on the anti-tumor mechanism of Astragalus polysaccharides. Front Oncol. 2024;14:1334915.
32. Sun S, Yang S, Zhang N, Yu C, Liu J, Feng W, Xu W, Mao Y. Astragalus polysaccharides alleviates cardiac hypertrophy in diabetic cardiomyopathy via inhibiting the BMP10-mediated signaling pathway. Phytomedicine. 2023;109:154543.
33. Jianwei X, Weijian Z, Xu C, Fanlian G, Xinpeng C, Yiwei H, Miaoyu Z, Zhizhong Y. Effect of Astragalus polysaccharides on the injury and apoptosis of rat chondrocytes induced by oxidative stress, J Clin Exp Med 2020;19(10):1040-1044.
34. Mattson MP. Dietary factors, hormesis and health. Ageing Res Rev. 2008;7(1):43-8.
35. Jie S, Gao Y, Sun H, Zhao H, Zhao Y, Chen C, Zeng H, Ma Y. Integrating network pharmacology and *in vivo* pharmacological investigation for deciphering the mechanism of Simiao Yong'an decoction in alleviating rheumatoid arthritis. Guidelines and Standards in Chinese Medicine. 2024;2(4):215-227.

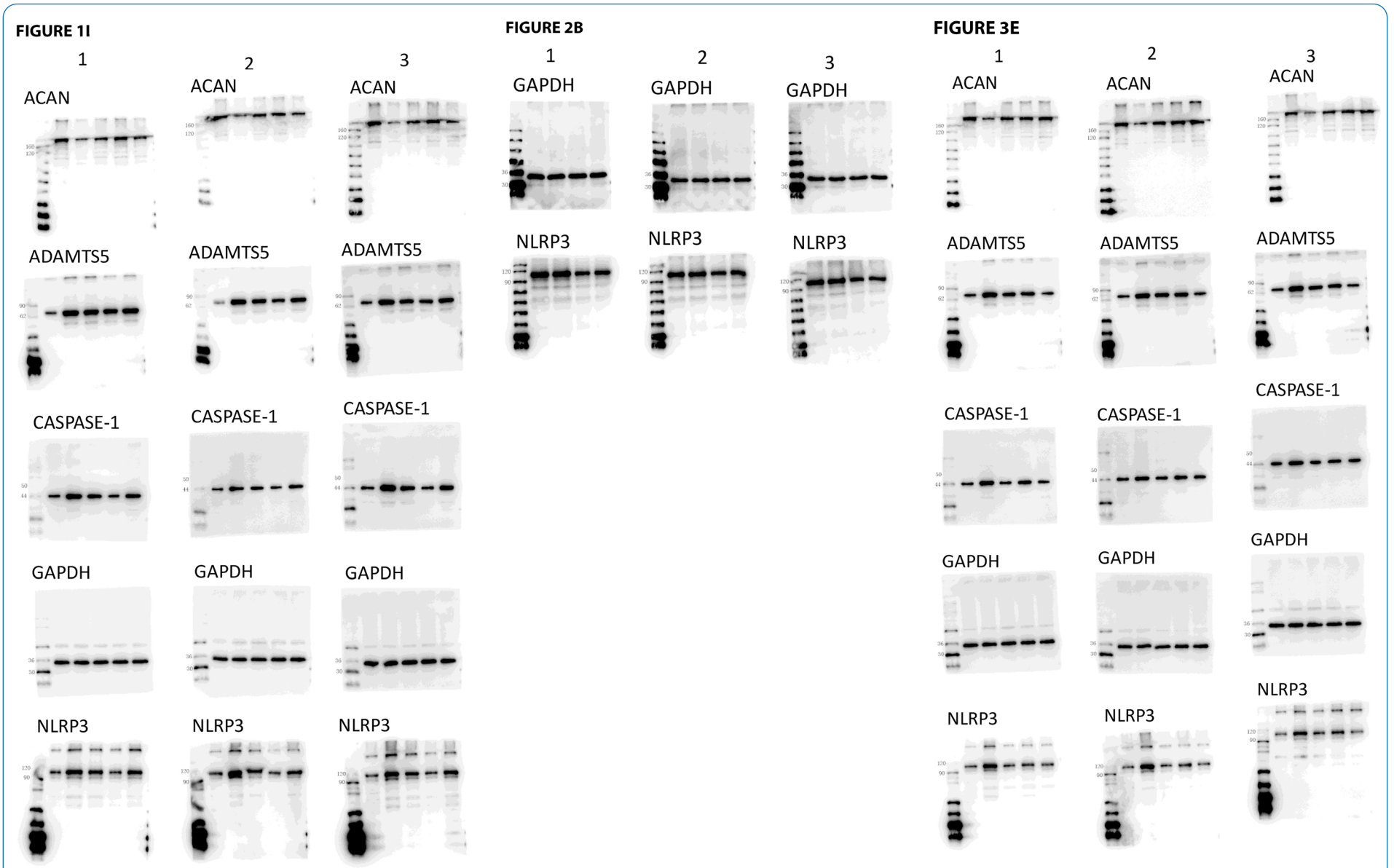

Supplementary Figure 1. Representative Western blot images (including molecular weight markers) for all quantified bands. Biological replicates 1–3 are shown.